

A modified spontaneous emulsification solvent diffusion method for the preparation of curcumin-loaded PLGA nanoparticles with enhanced *in vitro* anti-tumor activity

Cen CHEN^{1,2*}, Wei YANG^{1,2*}, Dan-Tong WANG^{1,2}, Chao-Long CHEN^{1,2}, Qing-Ye ZHUANG^{1,2},
and Xiang-Dong KONG (✉)^{1,2}

¹ Institute of Biomaterials and Marine Biological Resources, College of Life Sciences, Zhejiang Sci-Tech University, Hangzhou 310018, China

² Bio-X Center, Zhejiang Sci-Tech University, Hangzhou 310018, China

© Higher Education Press and Springer-Verlag Berlin Heidelberg 2014

ABSTRACT: To improve the anti-tumor activity of hydrophobic drug curcumin, we prepared curcumin-loaded PLGA nanoparticles (PLGA-Cur NPs) through a modified spontaneous emulsification solvent diffusion (modified-SESD) method. The influence of main preparation parameters was investigated, such as the volume ratio of binary organic solvents and the concentration of surfactant. Results indicated that the synthesized regular spherical PLGA NPs with the average diameter of 189.7 nm exhibited relatively higher yield (58.9%), drug loading (11.0% (w/w)) and encapsulation efficiency (33.5%), and also a controllable drug release profile. In order to evaluate the *in vitro* cytotoxicity of the prepared NPs, MTT assay was conducted, and results showed that the NPs could effectively inhibit HL60 and HepG2 cells with lower IC₅₀ values compared with free curcumin. Furthermore, confocal microscopy together with flow cytometry analysis proved the enhanced apoptosis-inducing ability of PLGA-Cur NPs. Polymeric NP formulations are potential to be used for hydrophobic drug delivery systems in cancer therapy.

KEYWORDS: curcumin; PLGA nanoparticle; modified spontaneous emulsification solvent diffusion (modified-SESD); anti-tumor

Contents

1	Introduction	2.4	Evaluation of curcumin release from NPs
2	Materials and methods	2.5	Cell culture
2.1	Materials	2.6	Cytotoxicity studies
2.2	Preparation of curcumin-loaded PLGA NPs	2.7	Investigation of cell apoptosis
2.3	Optimization and characterization of NPs	2.7.1	Confocal scanning laser microscopy
		2.7.2	Flow cytometry
		2.8	Statistical analysis
		3	Results
		3.1	Optimization of the PLGA-Cur NP formulation
		3.2	<i>In vitro</i> drug release of PLGA-Cur NPs
		3.3	Cell cytotoxicity assay

Received September 23, 2014; accepted October 22, 2014

E-mail: kongxiangdong@gmail.com

* C.C and W.Y. contributed equally to this work.

- 3.4 Morphological determination of apoptosis by confocal microscopy
- 3.5 Flow cytometric detection of apoptosis in HL60 cell line
- 4 Discussion
- 5 Conclusions
- Abbreviations
- Acknowledgements
- References

1 Introduction

Curcumin, extracted from the root of *Curcuma longa*, has attracted extensive researches in the past few decades due to its anti-inflammatory [1], antioxidant [2–3], antimicrobial [3] and especially anti-tumorigenic [4] activities. It has been demonstrated that curcumin exhibits inhibitory effect to a variety of cancers by anti-angiogenesis [4–5] and induction of tumor cell apoptosis [6–9].

Although possessing such excellent pharmacological activities, the therapeutic applications of curcumin are limited because of its poor water solubility, instability and relatively low bioavailability [10–11]. And the main approach to overcome these limitations is to introduce new drug delivery systems (DDSs) to curcumin [7]. The DDSs including liposomes [12], nanoparticles (NPs) [13–14], polymer micelles [4,15], hydrogels [16] and nanocrystal suspensions [17] not only improve the solubility and stability but also enhance drug targeting and bioavailability. Among all the DDSs, biodegradable polymeric NPs are extensively accepted as the promising therapeutic delivery for drugs and bioactive compounds [18–19].

Poly(lactic-*co*-glycolic acid) (PLGA) has been approved for clinical applications based on its biodegradability, biocompatibility and biosafety [20]. Lots of researches have mentioned the PLGA-encapsulated drug or protein NPs revealing better targeting property, bioavailability and low cytotoxicity [7,21–22], which encourage the formation of PLGA-curcumin (PLGA-Cur) NPs to improve the therapeutic value of curcumin.

The most widely used techniques for preparing PLGA NPs are nanoprecipitation technique [23], emulsification solvent evaporation (ESE) [24] and emulsification solvent diffusion (ESD) [25]. While compared with the other two, ESD, especially modified spontaneous emulsification solvent diffusion (modified-SESD) presents better properties such as high percentage of drug entrapment and narrow

size distribution [26].

In this work, modified-SESD was exploited to synthesize PLGA-Cur NPs, and the influence of various preparation parameters, including the volume ratio of organic solvents, the concentration of surfactant, the percentage of yield, the drug loading and the encapsulation content, were investigated to optimize the NPs formulation. Then PLGA-Cur NPs prepared by selected conditions were characterized for particle size, size distribution, and surface morphology. Furthermore, the *in vitro* curcumin release of PLGA-Cur NPs and its cytotoxicity in human leukemic HL60 cells and human hepatoma HepG2 cells were accomplished. Cell apoptosis which was induced by free curcumin or PLGA-Cur NPs was monitored through confocal scanning laser microscopy and flow cytometry with Annexin V-FITC/propidium iodide (PI) staining.

2 Materials and methods

2.1 Materials

PLGA (content ratio of lactic acid (LA) and glycolic acid (GA) 50:50, M_w 50 000) was purchased from Chengdu Institute of Organic Chemistry, Chinese Academy of Sciences. Curcumin was provided by Tongji Medical College, Huazhong University of Science and Technology (HUST). Ethylene (ETH), acetone (ACE), polyvinyl alcohol (PVA) and other reagents were purchased from Sigma-Aldrich. All chemicals and solvents were of reagent grade.

Human leukemic HL60 cells and human hepatoma HepG2 cells were obtained from Tongji Medical College, HUST. 3-(4,5)-Dimethylthiazolazo(-z-y1)-3,5-diphenyltetrazolium bromide (MTT) and Annexin V-FITC/PI assay kit were purchased from Beyotime Institute of Biotechnology. RPMI1640 media, fetal bovine serum (FBS), phosphate buffer solution (PBS), penicillin, and streptomycin were obtained from Gibco, Invitrogen.

2.2 Preparation of curcumin-loaded PLGA NPs

Curcumin-loaded PLGA NPs (PLGA-Cur NPs) were synthesized via the modified-SESD technique [27]. Briefly, 100 mg of PLGA was dissolved in ACE and 6 mg of free curcumin was dissolved in ETH. The total volume of organic solvents (ACE and ETH) was 5 mL with various volume ratios. The curcumin/ETH solution was added in a dropwise manner to the PLGA/ACE solution. This organic

phase was further added into 100 mL of aqueous PVA solution using a peristaltic pump at a flow rate of 2 mL/min with continuous stirring to solidify the NPs. The residual organic solvents were evaporated under negative pressure for 3 h and the NPs suspending were collected by ultracentrifugation at 12 000 r/min and washed with deionized water three times. Then the obtained products were lyophilized for 24 h. The NPs were stored at 4°C until further use.

2.3 Optimization and characterization of NPs

The prepared NPs differed along with varied organic solvent volume ratios and PVA concentrations. The percentage yield, contents of drug loading and encapsulation, particle size, size distribution, and surface morphology of the NPs were characterized to determine the formulation procedure.

The dried NPs were weighed and the yield (η) was calculated by using the following equation:

$$\eta/\% = \frac{w_{np}/g}{w_{dp}/g} \times 100 \quad (1)$$

where w_{np} is the weight of NPs obtained, and w_{dp} is the weight of drug and polymer used for NPs preparation.

Curcumin-loaded NPs (5 mg) were dissolved in 1 mL dimethyl sulfoxide (DMSO). The absorbance of curcumin in solution was measured at 450 nm by an ultraviolet (UV) spectrophotometer (HITACHI, U-2800). The curcumin concentration was calculated using a previously prepared standard curve of free curcumin. Drug loading and percentage encapsulation were given by:

$$\varphi_{dl}/\% = \frac{w_{ed}/g}{w_{pnp}/g} \times 100 \quad (2)$$

$$\varphi_e/\% = \frac{w_{ed}/g}{w_{dnp}/g} \times 100 \quad (3)$$

where, φ_{dl} and φ_e are contents of drug loading and encapsulation, respectively; w_{ed} is the weight of encapsulated drug in NPs; w_{pnp} is the weight of polymeric NPs; and w_{dnp} is the weight of drug used for NPs preparation.

The mean particle diameter and size distribution of PLGA-Cur NPs were determined by a dynamic light scattering (DLS) method using a Zetasizer Nano ZS (Malvern Instrument, UK). The shape and surface morphology of PLGA-Cur NPs were observed by scanning electron microscopy (SEM; JEOL, JSM-5610LV, Japan and FEI, Sirion 200, USA).

2.4 Evaluation of curcumin release from NPs

In vitro curcumin release kinetics of PLGA-Cur NPs was evaluated in phosphate buffer with 2% (v/v) ethanol since free curcumin is insoluble in aqueous solution. Briefly, 6 mg of lyophilized PLGA-Cur NPs were dispersed in 6 mL phosphate buffer with 2% ethanol. The samples were kept in a thermostatic water bath at 37°C with the stirring rate 100 r/min. At predetermined intervals, the supernatant was collected after centrifugation at 10 000 g for 5 min, and replaced with an equal volume of phosphate buffer with 2% ethanol. The concentration of released curcumin was measured by the UV spectrophotometer at 450 nm.

2.5 Cell culture

HL60 and HepG2 cells were cultured in RPMI 1640 media with 10% FBS, 100 IU/mL penicillin and 100 µg/mL streptomycin, in humidified atmosphere at 37°C with 5% CO₂. The cells were maintaining in the density range from 0.1 × 10⁶ to 1 × 10⁶ cells/mL. Logarithmic growth phase cells were used for experimental studies as required. Cells density was determined by a hemocytometer.

2.6 Cytotoxicity studies

To determine the effect of PLGA-Cur NPs on cell growth inhibition, MTT assay was performed. HL60 and HepG2 cells were suspended at a final concentration of 7 × 10⁴ cells/mL and seeded in 96-well plates. The cells were treated with 2.5, 5, 10, 20 and 40 µg/mL of free curcumin and equivalent doses of PLGA-Cur NPs. Cells cultured in absence of curcumin were used as control. After incubation for 24 or 48 h, MTT solutions (5 mg/mL) were added in each well and incubated at 37°C for 4 h. The precipitated formazan was dissolved in DMSO. Cells viability was evaluated by measuring the absorbance at 570 nm, using a microplate reader (Molecular Devices). Cell viability was expressed as percentage of curcumin-treated samples to control samples. The IC₅₀ value was directly calculated from the dose-response.

2.7 Investigation of cell apoptosis

During early apoptosis, phosphatidylserine (PS) is exposed from the inner to the outer leaflet of plasma membrane [28], and Annexin V-FITC has high affinity for binding PS residues. Furthermore, PI labels the late apoptotic/necrotic cells with membrane damage. On basis of this mechanism, double staining with Annexin V-FITC and PI were

employed to discriminate apoptotic cells from necrotic cells. HL60 and HepG2 cells were used to detect the apoptosis.

2.7.1 Confocal scanning laser microscopy

HepG2 cells (3×10^4 cells) were cultured on coverslips in 6-well plates. And after 12 h, the cells were treated with PLGA-Cur NPs (IC_{50} dose) for 3, 6, 12, 24 h, and untreated cells were used as control. After determined intervals, the cells were washed with PBS twice, and were incubated with 3 $\mu\text{g/mL}$ Annexin-FITC and 5 $\mu\text{g/mL}$ PI for 5 min in dark at room temperature. Then the cells were directly observed in a confocal scanning laser microscopy (Olympus).

2.7.2 Flow cytometry

HL60 cells were seeded within 24-well plates at a final concentration of 2.5×10^5 cells/mL, and then treated with PLGA-Cur NPs (IC_{50} dose) or equivalent doses of free curcumin for 3, 12, and 24 h. After determined intervals, cells were washed twice with PBS by centrifugation at 1000 r/min for 5 min, and resuspended in 500 μL binding buffer. Fluorescein isothiocyanate (FITC)-conjugated Annexin V (5 μL) and PI (5 μL) were added to each sample and the mixture was incubated at room temperature in the dark for 10 min. Then the cells were immediately analyzed by a fluorescence-activated cell sorter (FACS) using the Becton-Dickenson FC500 and Cell Quest software (Becton-Dickenson, Mountain View, CA, USA) to calculate the apoptosis percentage.

2.8 Statistical analysis

All quantitative data were depicted as the mean \pm standard deviation ($n = 3$). Tests of significance were performed using Student's *t*-test.

3 Results

3.1 Optimization of the PLGA-Cur NP formulation

The effects of process variables such as the volume ratio of binary organic solvents (ACE and ETH) and the PVA concentration on characteristics of PLGA-Cur NPs were investigated. As shown in Table 1, NPs prepared with binary organic solvents at the volume ratio $V(\text{ACE}):V(\text{ETH})$ of 1:1 resulted in the largest particle size and widest

Table 1 Effects of the volume ratio of organic solvents for PLGA-Cur NPs^{a)}

$V(\text{ACE}):V(\text{ETH})$	Average size /nm	Polydispersity index (PDI)
5:0	188.6	0.004
1:1	210.9	0.821
3:1	204.7	0.301
7:1	199.5	0.090
9:1	180.8	0.030

a) The preparation parameters: organic solvent mixture (5 mL), surfactant (2% w/v, PVA).

size distribution. In contrast, NPs prepared with $V(\text{ACE}):V(\text{ETH})$ of 9:1 displayed the smallest range of particle size with narrow size distribution. The influence of the PVA concentration on yield, drug loading and encapsulation content is illustrated in Table 2. The formulation was optimum at 3% PVA concentration with $V(\text{ACE}):V(\text{ETH})$ of 9:1. The yield, drug loading and encapsulation efficiency of the optimum batch of NPs were found to be 58.9%, 11.0% and 33.5%, respectively. Figure 1 shows the DLS result of PLGA-Cur NPs, depicting a narrow size distribution of the optimized batch with the mean particle size of 189.7 nm. Figure 2 shows the SEM image of NPs prepared with optimized conditions. Most NPs had regular spherical shape with smooth surfaces and without any aggregation.

Table 2 Effects of the PVA concentration for PLGA-Cur NPs^{a)}

PVA concentration /(% w/v)	Yield /%	Content of drug loading /%	Content of encapsulation /%
1	43.0	8.6	33.6
3	58.9	11.0	33.5
5	60.5	9.7	20.2

a) The preparation parameters: organic solvent mixture (5 mL), $V(\text{ACE}):V(\text{ETH}) = 9:1$.

3.2 *In vitro* drug release of PLGA-Cur NPs

The release kinetic of curcumin from PLGA-Cur NPs *in vitro* was studied for 15 d in phosphate buffer with 2% ethanol. As shown in Fig. 3, drug release follows a biphasic release manner — an initial burst, followed by a sustained curcumin release. During the initial release, about 10% of the encapsulated curcumin released from the NPs within 1 d. And after that, there was a constant slow release of curcumin, which released 48.8% of curcumin over 15 d.

3.3 Cell cytotoxicity assay

Cell cytotoxicity assays were carried out using equivalents dosages of free curcumin and PLGA-Cur NPs at

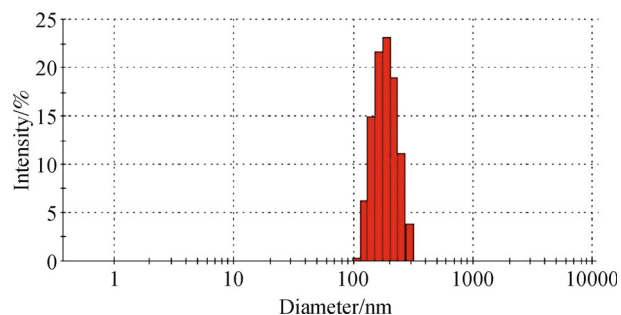


Fig. 1 DLS result of PLGA-Cur NPs: the mean particles diameter was found to be 189.7 nm.

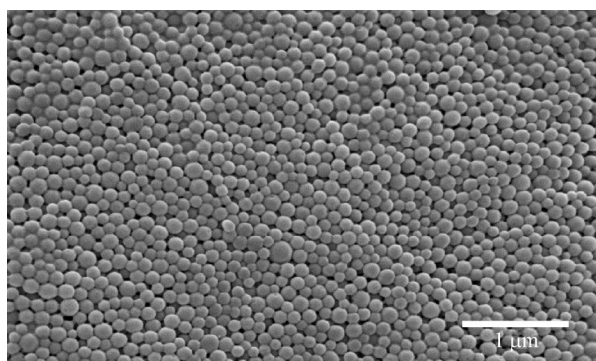


Fig. 2 SEM image of PLGA-Cur NPs with optimized batch formula.

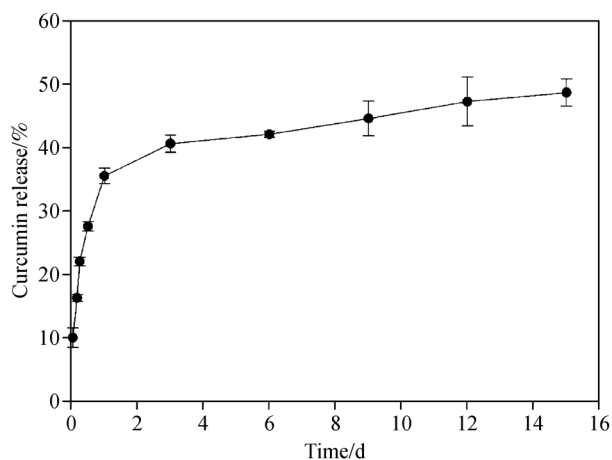


Fig. 3 *In vitro* release kinetic of curcumin from PLGA NPs in phosphate buffer with 2% ethanol over 15 d. All data were performed in triplicate, and given as mean \pm SD ($n = 3$).

concentrations of 0–40 $\mu\text{g}/\text{mL}$ to examine whether curcumin encapsulated in PLGA maintained its anticancer activity. The results of cell cytotoxicity on HL60 and HepG2 cells for 24 and 48 h are shown in Fig. 4, which indicate that free curcumin and PLGA-Cur NPs could inhibit cells growth of HL60 and HepG2 cells. The IC_{50} values of each group were shown in Table 3. The IC_{50} values of free curcumin were significantly higher than those of PLGA-Cur NPs against HL60 and HepG2 cells for 24 and 48 h, and the IC_{50} values of each condition against HL60 cells were lower than those against HepG2 cells.

3.4 Morphological determination of apoptosis by confocal microscopy

Exposed PS which is one of the early apoptotic features could be labeled by Annexin V-FITC [29]. And in late apoptotic or necrotic cells, some cells lost their membrane integrity and were characterized by chromatin compaction, nuclei fragmentation by the intercalating dye PI [30]. As shown in Fig. 5(a), cells of control group did not present any apoptotic features, and after exposed to PLGA-Cur NPs for 3 h, the HepG2 cells with integral membrane staining of Annexin V-FITC became visible (Fig. 5(b)). After 6 h, the ratio of cells with a profile of losing membrane integrity and nuclei stained red by PI increased as time progressed (Figs. 5(c)–5(e)). The arrows in Fig. 5 showed some of the nucleus that degenerated into discrete spherical fragments.

3.5 Flow cytometric detection of apoptosis in HL60 cell line

After treated with PLGA-Cur NPs (IC_{50} dose) and equivalent doses of free curcumin for 3, 12, and 24 h, HL60 cells were stained with Annexin V-FITC/PI and subjected to flow cytometry. Figure 6 shows the display of PI versus Annexin V-FITC. The lower left quadrants represent the viable (Annexin V $-$ /PI $-$) population, the lower right quadrants contain the apoptotic (Annexin V $+$ /PI $-$) population, the upper right quadrants stand for the necrotic and late apoptotic (Annexin V $+$ /PI $+$) population, and the upper left quadrants contain the damaged

Table 3 IC_{50} values of HL60 and HepG2 cells treated with free curcumin and PLGA-Cur NPs for different time

Time /h	IC_{50} value of HL60 /($\mu\text{g} \cdot \text{mL}^{-1}$)		IC_{50} value of HepG2 /($\mu\text{g} \cdot \text{mL}^{-1}$)	
	Free curcumin	PLGA-Cur NPs	Free curcumin	PLGA-Cur NPs
24	21.55	10.52	26.24	17.71
48	16.22	10.18	25.41	12.57

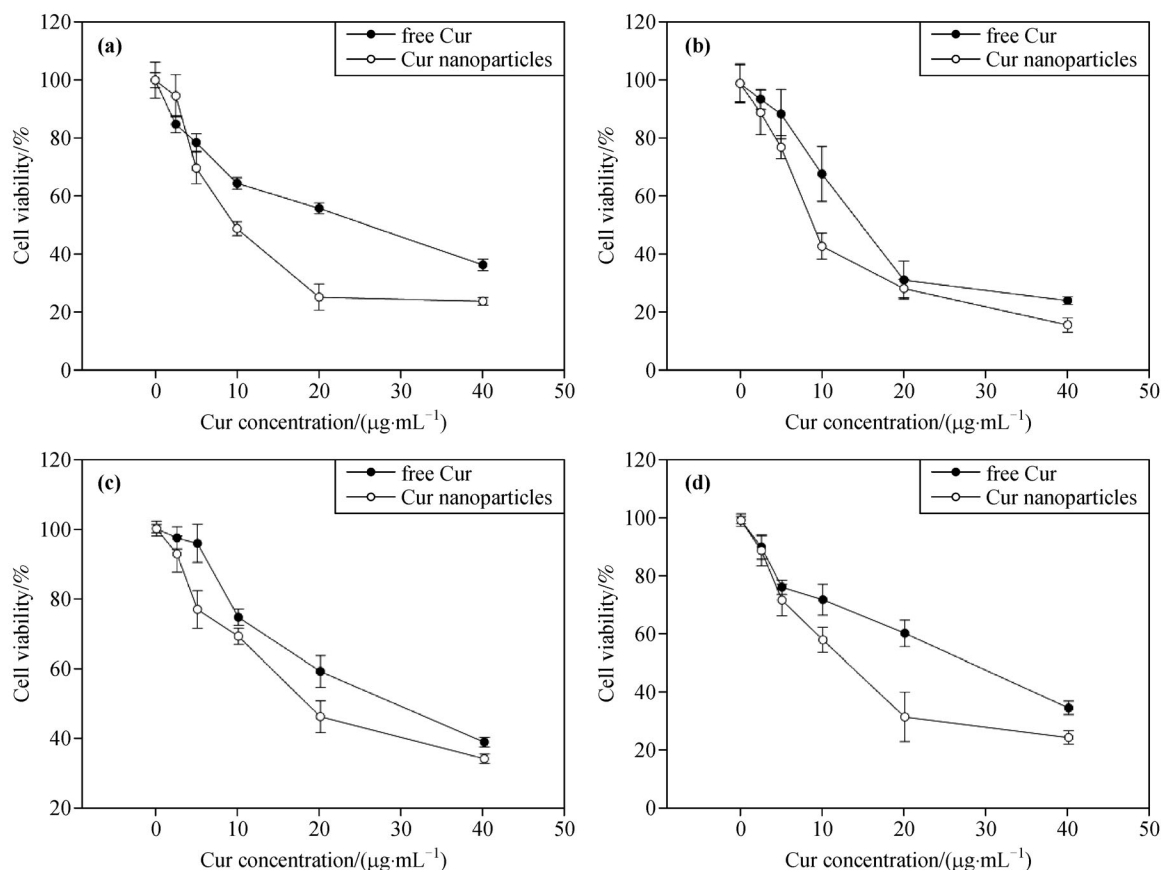


Fig. 4 Survival curves of HL60 cells after exposure to free curcumin and PLGA-Cur NPs for (a) 24 h and (b) 48 h, and survival curves of HepG2 cells after exposure to free curcumin and PLGA-Cur NPs for (c) 24 h and (d) 48 h.

(Annexin V-PI+) cells. Most of the cells were stained with Annexin V-FITC but not with PI and a few with both. The respective percentage of cells in viable, apoptotic, and necrotic phases are shown in Table 4. Treated HL60 cells with curcumin in solution or in NPs caused not only the increase of the number of early apoptotic cells, but also a progression into late apoptotic or necrotic cells. The proportions of apoptotic and necrotic cells treated with curcumin in NPs were higher than those treated with free curcumin at each time point.

4 Discussion

Curcumin has been proved to have favorable anti-tumorigenic activities due to its ability to inhibit angiogenesis and induce tumor cell apoptosis through downregulating various transcription factors as well as upregulating the expression of some antioncogenes [31]. However, poor aqueous solubility and bioavailability have limited its therapeutic applications. In the present study, we

prepared a biodegradable NP formulation of curcumin based on modified-SESD method. This method has been used to encapsulate a wide variety of drugs including etoposide [32], celecoxib [33], and furanodiene [34]. The most important challenge in formulation of a polymeric DDS involves preparing carrier which is capable to retain the biological activities of the encapsulated drug [35]. Characterization of the physicochemical properties of drug encapsulated within the NPs may possibly reveal useful information about the feasibility of using such a DDS for anticancer.

For effective passive targeting to cancerous tissues, drug-loaded NPs should be able to retain the drug and its biological activities for a prolonged time in circulation. *In vitro* drug release was carried out to measure the release kinetic of encapsulated curcumin in buffer. Drug release from PLGA NPs usually occurs in a biphasic manner, with an initial burst release followed by a sustained drug release. In our study, the rapid initial release (10% within 1 h) is attributed to the drug that adsorbed or weakly bound to the surface of NPs. A slower diffusion-controlled drug release

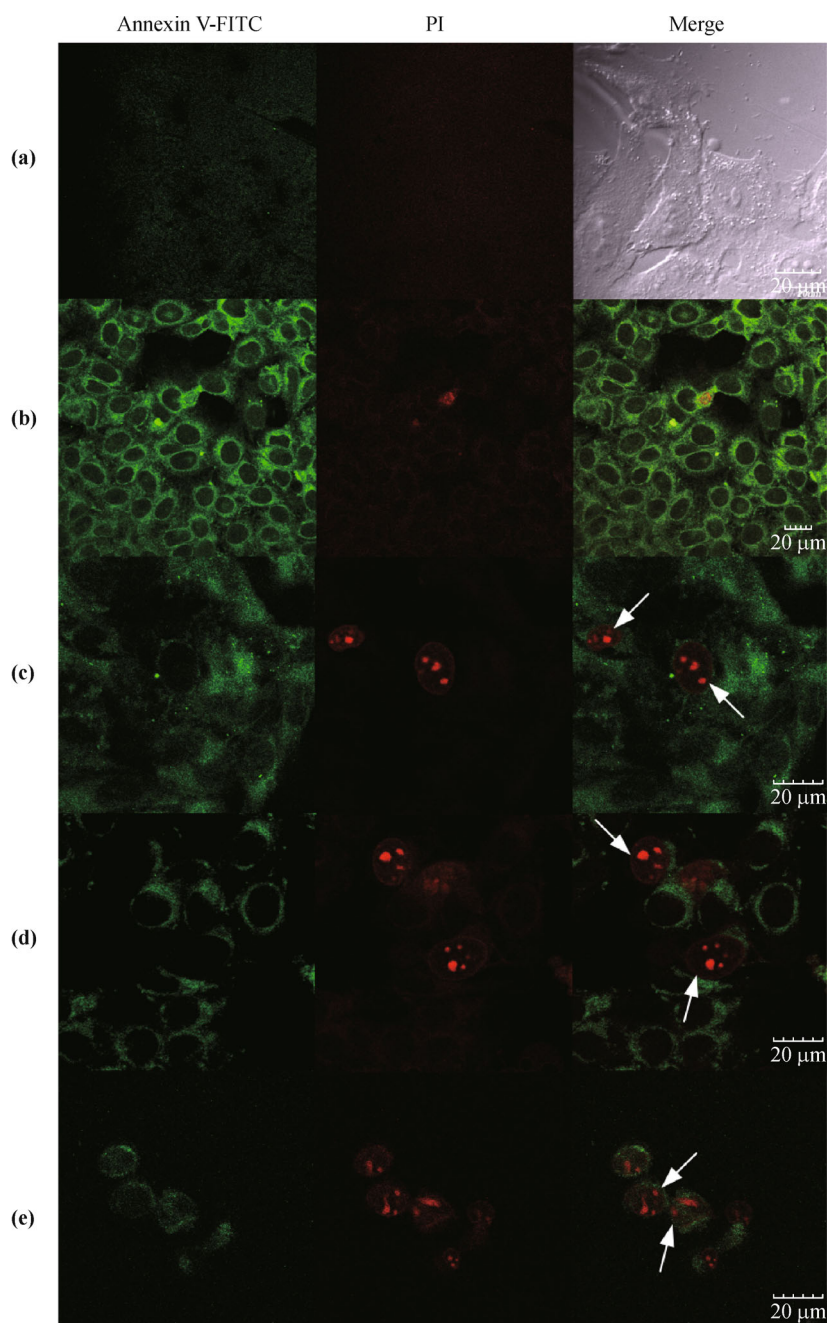


Fig. 5 Confocal microscopy images of (a) untreated HepG2 cells as control and treated with PLGA-Cur NPs (IC_{50} dose) for (b) 3 h, (c) 6 h, (d) 12 h, and (e) 24 h. Annexin V-FITC: green; PI: red; Merge: stack up images of Annexin V-FITC and PI.

of 48.8% was observed over 15 d due to the encapsulated curcumin in the NPs. To investigate the therapeutic potential of our PLGA-Cur NPs, HL60 and HepG2 cells were treated with free curcumin, and PLGA-Cur NPs at different concentrations (0–40 $\mu\text{g}/\text{mL}$) for 24 and 48 h. Free-Cur and PLGA-Cur NPs inhibited the growth of the tumor cells (HL60 and HepG2) in a dose-dependent manner. The results of the MTT assay confirmed that PLGA-Cur NPs exhibited a lower IC_{50} value in

comparison to free curcumin in both cancer cells we studied. Other studies of curcumin formulations have also shown that the encapsulated curcumin inhibited cancer cells proliferation comparably to free curcumin [36].

The ability to induce tumor cell apoptosis is an important feature of a candidate anticancer drug. The process of apoptosis is characterized by special biochemical and morphological changes. Membrane architecture changes leading to PS exposure occur rapidly in early apoptotic

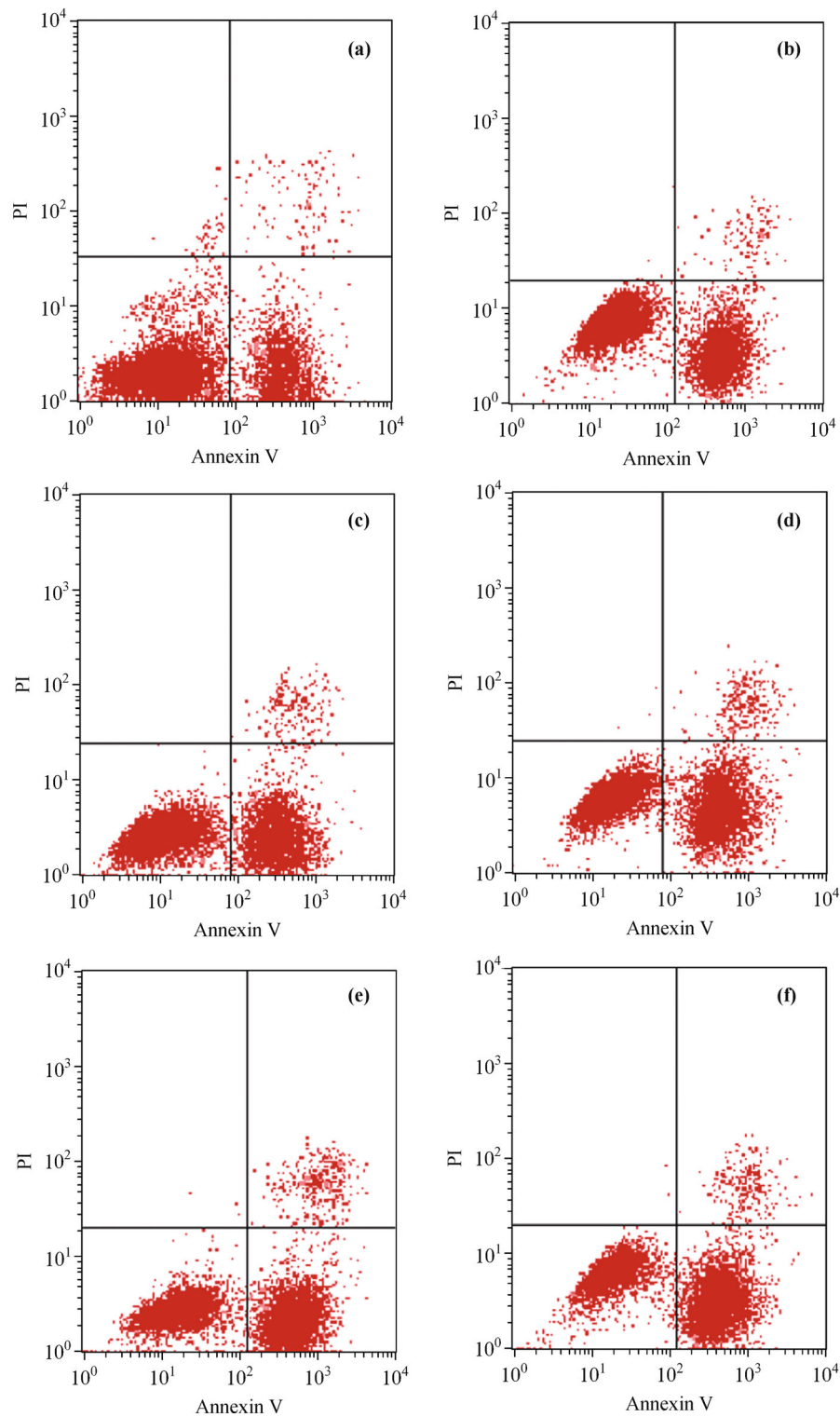


Fig. 6 Apoptotic cells detected by flow cytometer with double stained of Annexin V-FITC/PI. HL60 cells were treated with (a) free curcumin for 3 h, (b) PLGA-Cur NPs for 3 h, (c) free curcumin for 12 h, (d) PLGA-Cur NPs for 12 h, (e) free curcumin for 24 h, and (f) PLGA-Cur NPs for 24 h.

Table 4 Content of viable, apoptotic and necrotic cells of HL60 cells treated with free curcumin and PLGA-Cur NPs for different time

Cell phase	Content /%					
	Free curcumin, 3 h	PLGA-Cur NPs, 3 h	Free curcumin, 12 h	PLGA-Cur NPs, 12 h	Free curcumin, 24 h	PLGA-Cur NPs, 24 h
Viable	69.59	65.22	59.31	53.07	45.35	38.89
Apoptotic	28.69	33.24	38.56	43.89	50.74	58.32
Necrotic	1.25	1.47	2.13	3.04	3.88	2.76

cells, while the cells lose membrane integrity later in the apoptotic program and expose DNA [37]. So the apoptotic cells and necrotic cells can be examined by Annexin V-FITC/PI staining. In the present study, curcumin and PLGA-Cur NPs had obvious cytotoxic effect on HL60 and HepG2 cells at the concentration range of 2.5–40 $\mu\text{g}/\text{mL}$. Then morphological observation and flow cytometric analysis were carried out to explore whether the cytotoxic effect was related with apoptotic process. Confocal was used to observe the morphological changes of HepG2 cells with or without treatment of PLGA-Cur NPs. After the treatment for different intervals, a remarkable observation was that PS exposure seemed to precede the characteristic nuclear fragmentation during the process of apoptosis. Our flow cytometric analysis has shown that free curcumin and PLGA-Cur NPs treatment caused apoptosis in HL60 cell lines in a time-dependent manner. In comparison with free curcumin with poor solubility and stability, the PLGA-Cur NPs exhibited better effect of apoptosis induction to tumor cells.

5 Conclusions

In this study, the modified-SESD technique was used for the encapsulation of hydrophobic drug curcumin into PLGA NPs, which resulted in improved formulation characteristics including smaller size and narrow size distribution as well as high drug loading and encapsulation efficiency. In comparison with free curcumin, the PLGA-Cur NPs exhibited a controllable drug release profile, enhanced inhibition of cancer cells and lower IC_{50} against HL60 and HepG2 cells. All the results elucidate that optimized polymeric NP formulation are potential to be used for hydrophobic DDSs in cancer therapy.

Abbreviations

ACE	acetone
DDS	drug delivery system
DLS	dynamic light scattering

DMSO	dimethyl sulfoxide
ESD	emulsification solvent diffusion
ESE	emulsification solvent evaporation
ETH	ethylene
FACS	fluorescence-activated cell sorter
FBS	fetal bovine serum
FITC	fluorescein isothiocyanate
GA	glycolic acid
LA	lactic acid
MTT	3-(4,5)-dimethylthiazolyl-2,5-diphenyltetrazolium bromide
NP	nanoparticle
PBS	phosphate buffer solution
PI	propidium iodide
PLGA	poly(lactic-co-glycolic acid)
PLGA-Cur	PLGA-curcumin
PS	phosphatidylserine
PVA	polyvinyl alcohol
SEM	scanning electron microscopy
SESD	spontaneous emulsification solvent diffusion
UV	ultraviolet

Acknowledgements This work was supported by the National Natural Science Foundation of China (Grant Nos. 51272236 and 51002139), the Science Foundation of Zhejiang Sci-Tech University (Grant Nos. 13042158-Y, 0716687-Y and 0816833-Y), and the Zhejiang Provincial Top Key Discipline of Biology.

References

- [1] Heeba G H, Mahmoud M E, Hanafy A A. Anti-inflammatory potential of curcumin and quercetin in rats: Role of oxidative stress, heme oxygenase-1 and TNF- α . *Toxicology and Industrial Health*, 2012, 30(6): 551–560
- [2] Bhullar K S, Jha A, Youssef D, et al. Curcumin and its carbocyclic analogs: structure–activity in relation to antioxidant and selected biological properties. *Molecules*, 2013, 18(5): 5389–5404
- [3] Zemljic L F, Volmajer J, Ristic T, et al. Antimicrobial and antioxidant functionalization of viscose fabric using chitosan–curcumin formulations. *Textile Research Journal*, 2014, 84(8): 819–830
- [4] Gong C, Deng S, Wu Q, et al. Improving antiangiogenesis and anti-tumor activity of curcumin by biodegradable polymeric

- micelles. *Biomaterials*, 2013, 34(4): 1413–1432
- [5] Fan X, Zhang C, Liu D B, et al. The clinical applications of curcumin: current state and the future. *Current Pharmaceutical Design*, 2013, 19(11): 2011–2031
- [6] Liu H, Liu Y Z, Zhang F, et al. Identification of potential pathways involved in the induction of cell cycle arrest and apoptosis by a new 4-arylidene curcumin analogue T63 in lung cancer cells: a comparative proteomic analysis. *Molecular BioSystems*, 2014, 10(6): 1320–1331
- [7] Verderio P, Bonetti P, Colombo M, et al. Intracellular drug release from curcumin-loaded PLGA nanoparticles induces G2/M block in breast cancer cells. *Biomacromolecules*, 2013, 14(3): 672–682
- [8] Ono M, Higuchi T, Takeshima M, et al. Differential anti-tumor activities of curcumin against Ras- and Src-activated human adenocarcinoma cells. *Biochemical and Biophysical Research Communications*, 2013, 436(2): 186–191
- [9] Chang Z, Xing J, Yu X. Curcumin induces osteosarcoma MG63 cells apoptosis via ROS/Cyto-C/Caspase-3 pathway. *Tumor Biology*, 2014, 35(1): 753–758
- [10] Li B, Konecke S, Wegiel L A, et al. Both solubility and chemical stability of curcumin are enhanced by solid dispersion in cellulose derivative matrices. *Carbohydrate Polymers*, 2013, 98(1): 1108–1116
- [11] Rachmawati H, Al Shaal L, Müller R H, et al. Development of curcumin nanocrystal: physical aspects. *Journal of Pharmaceutical Sciences*, 2013, 102(1): 204–214
- [12] Barui S, Saha S, Mondal G, et al. Simultaneous delivery of doxorubicin and curcumin encapsulated in liposomes of pegylated RGDK-lipopeptide to tumor vasculature. *Biomaterials*, 2014, 35(5): 1643–1656
- [13] Zhao R B, Yang X Y, Chen C, et al. The anti-tumour effect of p53 gene loaded hydroxyapatite nanoparticles *in vitro* and *in vivo*. *Journal of Nanoparticle Research*, 2014, 16(4): 2353–2367
- [14] Chuah L H, Roberts C J, Billa N, et al. Cellular uptake and anticancer effects of mucoadhesive curcumin-containing chitosan nanoparticles. *Colloids and Surfaces B: Biointerfaces*, 2014, 116: 228–236
- [15] Nakayama M, Akimoto J, Okano T. Polymeric micelles with stimuli-triggering systems for advanced cancer drug targeting. *Journal of Drug Targeting*, 2014, 22(7): 584–599
- [16] Ma J, Yang F, Both S K, et al. Comparison of cell-loading methods in hydrogel systems. *Journal of Biomedical Materials Research Part A*, 2014, 102(4): 935–946
- [17] Ravichandran R. Studies on dissolution behaviour of nanoparticulate curcumin formulation. *Advances in Nanoparticles*, 2013, 2(1): 51–59
- [18] Ye F, Barrefelt A, Asem H, et al. Biodegradable polymeric vesicles containing magnetic nanoparticles, quantum dots and anticancer drugs for drug delivery and imaging. *Biomaterials*, 2014, 35(12): 3885–3894
- [19] Guerrero-Cázares H, Tzeng S Y, Young N P, et al. Biodegradable polymeric nanoparticles show high efficacy and specificity at DNA delivery to human glioblastoma *in vitro* and *in vivo*. *ACS Nano*, 2014, 8(5): 5141–5153
- [20] Danhier F, Ansorena E, Silva J M, et al. PLGA-based nanoparticles: an overview of biomedical applications. *Journal of Controlled Release*, 2012, 161(2): 505–522
- [21] Cui Y, Xu Q, Chow P K H, et al. Transferrin-conjugated magnetic silica PLGA nanoparticles loaded with doxorubicin and paclitaxel for brain glioma treatment. *Biomaterials*, 2013, 34(33): 8511–8520
- [22] Paul A, Das S, Das J, et al. Cytotoxicity and apoptotic signalling cascade induced by chelidone-loaded PLGA nanoparticles in HepG2 cells *in vitro* and bioavailability of nano-chelidone in mice *in vivo*. *Toxicology Letters*, 2013, 222(1): 10–22
- [23] Yang Z, Luo X, Zhang X, et al. Targeted delivery of 10-hydroxycamptothecin to human breast cancers by cyclic RGD-modified lipid-polymer hybrid nanoparticles. *Biomedical Materials*, 2013, 8(2): 025012
- [24] Xiong S, Zhao X, Heng B C, et al. Cellular uptake of Poly-(D,L-lactide-co-glycolide) (PLGA) nanoparticles synthesized through solvent emulsion evaporation and nanoprecipitation method. *Biotechnology Journal*, 2011, 6(5): 501–508
- [25] Xu A, Yao M, Xu G, et al. A physical model for the size-dependent cellular uptake of nanoparticles modified with cationic surfactants. *International Journal of Nanomedicine*, 2012, 7: 3547–3554
- [26] Ye Z, Squillante E. The development and scale-up of biodegradable polymeric nanoparticles loaded with ibuprofen. *Colloids and Surfaces A: Physicochemical and Engineering Aspects*, 2013, 422(5): 75–80
- [27] Murakami H, Kobayashi M, Takeuchi H, et al. Further application of a modified spontaneous emulsification solvent diffusion method to various types of PLGA and PLA polymers for preparation of nanoparticles. *Powder Technology*, 2000, 107(1–2): 137–143
- [28] Fadok V A, Bratton D L, Frasch S C, et al. The role of phosphatidylserine in recognition of apoptotic cells by phagocytes. *Cell Death and Differentiation*, 1998, 5(7): 551–562
- [29] Wang H, Tang X, Tang G, et al. Noninvasive positron emission tomography imaging of cell death using a novel small-molecule probe, (18)F labeled bis(zinc(II)-dipicolylamine) complex. *Apoptosis*, 2013, 18(8): 1017–1027
- [30] Darzynkiewicz Z, Bruno S, Del Bino G, et al. Features of apoptotic cells measured by flow cytometry. *Cytometry*, 1992, 13(8): 795–808
- [31] Kamat A M, Tharakan S T, Sung B, et al. Curcumin potentiates the

- antitumor effects of Bacillus Calmette-Guerin against bladder cancer through the downregulation of NF- κ B and upregulation of TRAIL receptors. *Cancer Research*, 2009, 69(23): 8958–8966
- [32] Callewaert M, Dukic S, Van Gulick L, et al. Etoposide encapsulation in surface-modified poly(lactide-co-glycolide) nanoparticles strongly enhances glioma antitumor efficiency. *Journal of Biomedical Materials Research Part A*, 2013, 101A(5): 1319–1327
- [33] Ibrahim M M, Abd-Elgawad A E H, Soliman O A E, et al. Nanoparticle-based topical ophthalmic formulations for sustained celecoxib release. *Journal of Pharmaceutical Sciences*, 2013, 102(3): 1036–1053
- [34] Li G, Lin D H, Xie X X, et al. Uptake and transport of furanodiene in Caco-2 cell monolayers: a comparison study between furanodiene and furanodiene loaded PLGA nanoparticles. *Chinese Journal of Natural Medicine*, 2013, 11(1): 49–55
- [35] Zhang Y, Chan H F, Leong K W. Advanced materials and processing for drug delivery: the past and the future. *Advanced Drug Delivery Reviews*, 2013, 65(1): 104–120
- [36] Kumar S S D, Surianarayanan M, Vijayaraghavan R, et al. Curcumin loaded poly(2-hydroxyethyl methacrylate) nanoparticles from gelled ionic liquid — *in vitro* cytotoxicity and anticancer activity in SKOV-3 cells. *European Journal of Pharmaceutical Sciences*, 2014, 51: 34–44
- [37] Henry C M, Hollville E, Martin S J. Measuring apoptosis by microscopy and flow cytometry. *Methods*, 2013, 61(2): 90–97